

The heat capacities of LiNO_3 and CsNO_3 from 350 to 700 K

M.J. Maeso ^a and J. Largo ^{b,*}

^a *Departamento de Física Aplicada, Universidad de Cantabria, 39005 Santander (Spain)*

^b *Departamento de Ingeniería Eléctrica y Energética, Universidad de Cantabria, 39005 Santander (Spain)*

(Received 26 October 1992; accepted 15 November 1992)

Abstract

The heat capacities of LiNO_3 and CsNO_3 were determined from 350 to 700 K by differential scanning calorimetry. For CsNO_3 , a solid–solid transition was observed at 426.5 K and the entropy associated with this transition was found to be $8.32 \text{ J K}^{-1} \text{ mol}^{-1}$. At 298.15 K, the values of C_p^\ominus , S_T^\ominus , $[H^\ominus(T) - H^\ominus(0)]/T$ and $-[G^\ominus(T) - H^\ominus(0)]/T$ respectively, are 89.95, 52.65, 96.47 and $38.6 \text{ J K}^{-1} \text{ mol}^{-1}$ for LiNO_3 and 96.47, 67.23, 153.95 and $86.71 \text{ J K}^{-1} \text{ mol}^{-1}$ for CsNO_3 . Values for $[H^\ominus(T) - H^\ominus(0)]/T$, $[S^\ominus(T) - S^\ominus(0)]$ and $-[G^\ominus(T) - H^\ominus(0)]/T$ for LiNO_3 and CsNO_3 from 350 to 700 K were calculated and tabulated.

INTRODUCTION

There is a large amount of data published on the molten alkaline metal nitrates XNO_3 (where X is Li, Na, K, Cs, Tl) because thermal energy storage is of increasing importance in the field of energy technology. Because LiNO_3 , NaNO_3 etc., and their binary mixtures, are considered to be possible latent-heat storage materials at medium temperatures, it is necessary to determine the thermodynamic properties of these salts through fusion.

This work was performed to determine the heats of transition and fusion, and the specific heats of the solid and liquid phases of the nitrates LiNO_3 and CsNO_3 . These values were used to determine the properties of these nitrates from 350 to 700 K.

EXPERIMENTAL

The salts used were pure-grade recrystallized reagents, dried at 400 K under vacuum until use. The heat capacity measurements were made with a Perkin-Elmer DSC-II differential scanning calorimeter at a heating rate of

* Corresponding author.

10–20°C min⁻¹, with range settings of 1.25–5.00 J min⁻¹. The heat capacity reference material used was sapphire.

Measurements were processed on a desk-top calculator which controlled the calorimeter. The heat capacity values were an average of three recorded at each temperature. Measurement accuracies in the solid regions were estimated to be 2% in comparison with previous heat capacity results. In the liquid region, they are estimated to be 4%.

RESULTS AND DISCUSSION

The melting temperature and enthalpy of fusion were found to be 527.5 K and 24.5 J K⁻¹ mol⁻¹, respectively, for LiNO₃, and for CsNO₃, the temperature and enthalpy of transition were 426.5 K and 3.8 J K⁻¹ mol⁻¹ and the temperature and enthalpy of fusion were 678.2 K and 15.5 J K⁻¹ mol⁻¹, respectively. These values are given in Tables 1 and 2, respectively. There is no evidence of changes in the thermodynamic properties of LiNO₃ between room temperature and the melting temperature. In most previous studies on the enthalpy of fusion, the results are not very accurate because of the hygroscopic nature of LiNO₃.

The measured molar heat capacities for LiNO₃ and CsNO₃ are given in Tables 3 and 4, and are shown in Figs. 1 and 2. The average heat capacities for both solid and liquid phases were calculated and are given in Tables 5 and 6. The temperature range over which the value of C_p was obtained is shown in parentheses. The values for solid LiNO₃ are higher than those determined by adiabatic calorimetry [1, 4], but are comparable with those

TABLE 1
Temperature and heat of fusion of LiNO₃

T_f /K	$\Delta_f H/(kJ mol^{-1})$	Ref.
527.5	24.5	This work
525	36.7	1
526.3	26.7	2
525	25.5	3
525	24.6	4

TABLE 2
Temperature and heat of transition and fusion CsNO₃

T_{tr} /K	$\Delta_{tr} H/(kJ mol^{-1})$	T_f /K	$\Delta_f H/(kJ mol^{-1})$	Ref.
426.5	3.8	678.2	15.5	This work
427.4	3.72	678	14.1	5
425	3.7	679	14.1	6

TABLE 3

Heat capacity of LiNO₃

<i>T</i> /K	<i>C_p</i> /(J K ⁻¹ mol ⁻¹)	<i>T</i> /K	<i>C_p</i> /(J K ⁻¹ mol ⁻¹)	<i>T</i> /K	<i>C_p</i> /(J K ⁻¹ mol ⁻¹)
350	88.7	512	135.0	539	136.7
360	90.3	513	136.6	540	136.6
370	91.9	514	141.1	541	136.6
380	93.5	515	143.6	542	136.3
390	95.5	516	148.1	543	136.5
400	97.3	517	155.2	544	136.7
410	99.1	518	160.5	545	136.2
420	101.2	519	175.7	546	136.6
430	103.3	520	227.8	547	136.5
440	105.7	521	283.2	548	136.6
450	107.4	522	315.6	549	137.1
460	108.1	523	378.9	550	136.6
470	110.2	524	574.8	560	137.6
480	111.8	525	712.3	570	138.3
490	114.3	526	999.0	580	139.1
500	118.7	527	1852.0	590	139.5
501	119.3	528	2340.0	600	140.3
502	120.8	529	3120.0	610	140.6
503	122.1	530	4360.0	620	140.3
504	122.2	531	–	630	140.5
505	123.1	532	4480.0	640	140.7
506	123.3	533	507.1	650	140.5
507	124.7	534	263.8	660	140.6
508	126.7	535	143.5	670	140.5
509	126.9	536	138.3	680	140.7
510	129.8	537	137.2	690	140.5
511	131.4	538	136.9	700	140.6

found by Ichikawa and Matsumoto [8]; for the liquid phase, the heat capacity is lower than all previously reported values.

The heat capacity values of CsNO₃ in the solid and liquid regions are not in good agreement with those published. We believe that the values obtained here are correct because differential scanning calorimetry yields heat capacity values for NaNO₃ and KNO₃ that are similar to those obtained by Carling [9].

The change in the heat capacity on fusion at T_{mp} $\Delta C_p(T_{mp})$ is given as the difference between the heat capacities just below T_{mp} and immediately above T_{mp} , between which the experimental values show the peak of C_p . Thus, $\Delta C_p(T_{mp})$ may be defined by

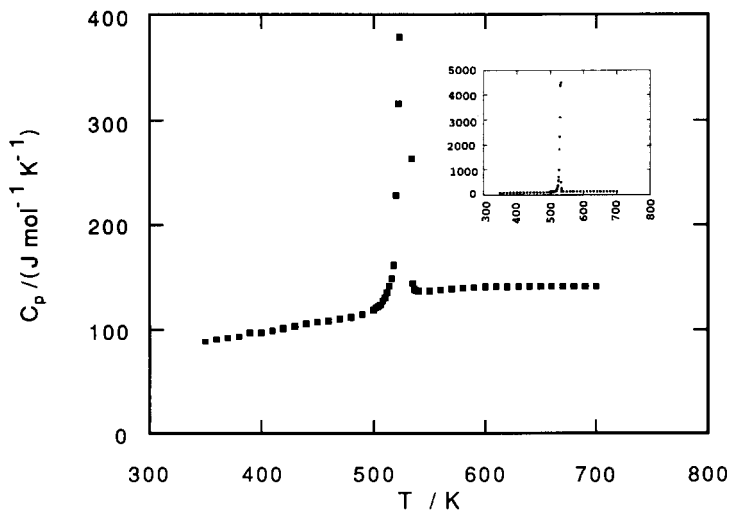
$$\Delta C_p(T_{mp}) = \lim_{\delta \rightarrow 0} [C_p^L(T_{mp} + \delta)] - \lim_{\delta' \rightarrow 0} [C_p^S(T_{mp} - \delta')]$$

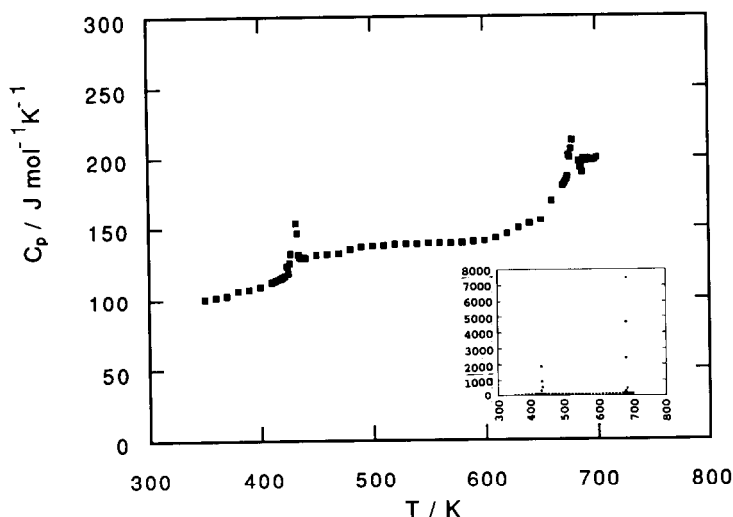
where δ and δ' are positive.

TABLE 4

Heat capacity of CsNO₃

T/K	$C_p/$ ($\text{J K}^{-1} \text{mol}^{-1}$)	T/K	$C_p/$ ($\text{J K}^{-1} \text{mol}^{-1}$)	T/K	$C_p/$ ($\text{J K}^{-1} \text{mol}^{-1}$)
350	100.4	433	146.5	660	169.2
360	101.5	434	131.3	670	180.0
370	102.7	435	129.5	671	181.2
380	106.1	436	129.2	672	182.5
390	106.9	437	129.0	673	184.3
400	108.9	438	128.9	674	186.3
410	111.9	439	129.1	675	201.4
411	111.4	440	128.8	676	199.8
412	112.5	450	131.1	677	205.8
413	112.9	460	131.6	678	212.1
414	113.2	470	133.2	679	328.8
415	113.6	480	135.0	680	2414.9
416	113.9	490	136.7	681	4658.0
417	114.2	500	137.2	682	7470.0
418	114.5	510	137.5	683	523.0
419	114.7	520	138.3	684	197.3
420	115.3	530	138.6	685	192.8
421	115.9	540	138.5	686	192.8
422	116.5	550	139.2	687	189.6
423	118.5	560	139.3	688	199.3
424	123.1	570	138.9	689	196.7
425	118.1	580	139.4	690	197.5
426	125.4	590	140.2	691	198.3
427	132.0	600	140.7	692	199.2
428	367.3	610	142.6	693	199.5
429	1864.0	620	145.6	694	198.6
430	937.2	630	149.6	695	198.2
431	584.0	640	152.7	696	197.9
432	153.5	650	155.2	700	199.6

Fig. 1. Experimental heat capacity of LiNO₃.

Fig. 2. Experimental heat capacity of CsNO_3 .

The heat capacities were fitted to polynomials as a function of temperature by the method of least-squares, and integrated to yield smoothed values of the thermodynamic functions at selected temperature intervals. In the vicinity of the transitions, the thermal functions are based on numerical integration of the heat capacities values read from a plot of the transition and melting regions. The values are based on molar masses of

TABLE 5

Heat capacities of solid and liquid LiNO_3

Ref.	$C_p(\text{s})/(\text{J K}^{-1} \text{mol}^{-1})$	$C_p(\text{l})/(\text{J K}^{-1} \text{mol}^{-1})$
This work	118.0	136.5
2	106 (433 K)	150 (523 K)
4	111 (442–525 K)	152 (527–576 K)
7	105 (299–525 K)	148 (525–552 K)
8	116.5 (350–515 K)	139.7 (550–675 K)

TABLE 6

Heat capacities of solid and liquid CsNO_3

Ref.	$C_p(\text{s})\text{I}/$ $(\text{J K}^{-1} \text{mol}^{-1})$	$C_p(\text{s})\text{II}/$ $(\text{J K}^{-1} \text{mol}^{-1})$	$C_p(\text{l})/$ $(\text{J K}^{-1} \text{mol}^{-1})$
This work	113	140	197
6	113 (400 K)	135–168 (450–675 K)	173 (700 K)
8	125 (300–425 K)	147 (450–670 K)	142 (679–700 K)

TABLE 7

Standard molar thermodynamic functions of LiNO_3

T/K	$C_p/$ ($\text{J K}^{-1} \text{mol}^{-1}$)	$S^\ominus(T) - S^\ominus(0)/$ ($\text{J K}^{-1} \text{mol}^{-1}$)	$[H^\ominus(T) - H^\ominus(0)]/T/$ ($\text{J K}^{-1} \text{mol}^{-1}$)	$-[G^\ominus(T) - H^\ominus(0)]/T/$ ($\text{J K}^{-1} \text{mol}^{-1}$)
350	88.7	58.6	100.1	41.4
360	90.3	59.4	102.6	43.1
380	93.5	61.2	107.6	46.4
400	97.3	62.9	112.5	49.5
420	101.2	64.6	117.3	52.7
440	105.7	66.4	122.1	55.7
460	108.1	68.1	126.9	58.7
480	111.8	69.9	131.6	61.6
500	118.7	71.7	136.3	64.6
550	136.6	120.2	192.1	71.8
560	137.6	120.5	194.6	74.1
580	139.1	121.1	199.4	78.2
600	140.3	121.7	204.2	82.4
620	140.3	122.3	208.8	86.5
640	140.7	122.9	213.2	90.2
660	140.6	123.4	217.6	94.1
680	140.7	123.9	221.8	97.8
700	140.6	124.4	225.8	101.3

TABLE 8

Standard molar thermodynamic functions of CsNO_3

T/K	$C_p/$ ($\text{J K}^{-1} \text{mol}^{-1}$)	$S^\ominus(T) - S^\ominus(0)/$ ($\text{J K}^{-1} \text{mol}^{-1}$)	$[H^\ominus(T) - H^\ominus(0)]/T/$ ($\text{J K}^{-1} \text{mol}^{-1}$)	$-[G^\ominus(T) - H^\ominus(0)]/T/$ ($\text{J K}^{-1} \text{mol}^{-1}$)
350	100.4	72.2	170.0	97.9
360	101.5	72.9	172.9	99.9
370	102.7	73.7	175.7	101.9
380	106.9	74.5	178.4	103.9
390	106.9	75.3	181.2	105.8
400	108.9	76.1	183.9	107.8
450	131.1	85.7	202.4	116.7
460	131.6	86.7	205.3	118.6
470	133.2	87.7	208.2	120.5
480	135.0	85.6	211.0	125.4
490	136.7	89.6	213.8	124.1
500	137.2	90.6	219.2	128.6
520	138.3	92.4	224.4	132.0
540	138.5	94.1	229.5	135.3
560	139.3	95.7	234.4	138.6
580	139.4	97.2	239.3	142.0
600	140.7	98.7	244.1	145.4
620	145.6	101.1	248.8	148.7
640	152.7	101.6	251.2	149.5
650	155.2	102.5	253.8	151.3

68.95 and 194.91 g mol⁻¹ for LiNO₃ and CsNO₃, respectively. Values for standard enthalpy and entropy (J K⁻¹ mol⁻¹) at 298.15 K are 15700 and 100.0 for LiNO₃ [10], and 20046 and 153.95 for CsNO₃ [11], respectively (Tables 7 and 8).

The solid–solid transition in CsNO₃ involves a discontinuous change from one crystal structure (pseudohexagonal **II**) to another (cubic **I**) at 426.5 K. The difference in structure between phases **I** and **II** is due to changes in the orientation of the NO₃⁻ ion, the position of the Cs⁺ ion being practically the same [12]. The entropy of transition determined in this work is 8.32 J K⁻¹ mol⁻¹ which is reasonably close to the theoretical value ($R \ln 3$) and lends credence to the interpretation of the mechanisms of the transition described by Newns and Staveley [13].

REFERENCES

- 1 R.P. Tye, A.O. Dresjarlais and J.G. Bourne, in A. Cezairiliyan (Ed.), Proc. 7th Symp. Thermophysical Properties, American Society of Mechanical Engineers, 1977, p. 189.
- 2 C. Sinistri and P. Franzosini, Ric. Sci. Parte 2, Sez. A., 33 (1963) 419.
- 3 H.M. Goodwin and H.T. Kalmus, Phys. Rev., 28 (1909) 1.
- 4 M. Kamimoto, T. Tanaka, T. Tani and T. Horigome, Sol. Energy, (1980) 24.
- 5 K.H. Stern, J. Phys. Chem. Ref. Data., 1 (1972) 747.
- 6 A. Mustajoki, Ann. Acad. Sci. Fenn. Ser. A, 6 (1962) 99.
- 7 P. Chevin, W.C. Hamilton and B. Post, Acta Crystallogr., 23 (1967) 55.
- 8 K. Ichikawa and T. Matsumoto, Bull. Chem. Soc. Jpn., 56 (1983) 2093.
- 9 R.W. Carling, Thermochim. Acta, 60 (1983) 265.
- 10 CODATA Recommended Key Values for Thermodynamics, 1977, J. Chem. Thermodyn., (10 (1978) 903.
- 11 H.E. Flotow, P.A.G. O'Hare and J. Boerio-Goates, J. Chem. Thermodyn., 13 (1981) 477.
- 12 F. Ferroni, A. Sabatini and P. Orioli, Ric. Sci., 27 (1957) 1557.
- 13 D.M. Newns and L.A. Staveley, Chem. Rev., 66 (1966) 267.